Solvent Effects on Electronic Spectra at Liquid Interfaces. A Continuum Electrostatic Model

Ilan Benjamin

Department of Chemistry, University of California, Santa Cruz, California 95064

Received: April 29, 1998; In Final Form: June 17, 1998

The electronic absorption line shape of a model chromophore at liquid interfaces is numerically evaluated using electrostatic continuum theory. The interface is described as a sharp boundary separating two bulk media, each characterized by different optical and static dielectric constant. The chromophore is modeled as a pair of spherical cavities in which two equal and opposite point charges are embedded, but more complicated charge distributions are possible. All possible orientations of the two cavities relative to the interface are properly weighted, including the cases where each cavity may be located in both phases. Comparisons are made with experiments, approximate analytical results, and molecular dynamics simulations.

I. Introduction

Solvent effects on electronic spectra have been extensively studied in order to understand the nature of the condensed phase environment and its effect on the structure and dynamics of solute molecules.[1] The shift in the position of the peak spectrum taken in a given solvent relative to the spectrum in the gas phase provides information about the polarity of the solvent and about specific solute/solvent interactions. The shift of the spectra of selected chromophores relative to the spectrum in a bulk reference solvent has been used to construct very useful empirical solvent polarity scales.[2] Various theoretical approaches have been used to understand the effect of bulk liquids on electronic spectra.[3−7] Continuum electrostatic models have been used to derive expressions for the position of the peak spectra.[8,9] These expressions are useful for extracting solute properties[10−12] (such as excited state dipole moments) from the wealth of available experimental data.

In recent years, due to advances in experimental techniques such as non-linear optical spectroscopies, measurements of electronic spectra in complex environments such as that of liquid interfaces have been reported. For example, the polarity of the micelle−water interface has been probed by Saroja and Samanta using a solvent-sensitive fluorescence probe.[13] Girault and coworkers have measured the electronic spectrum of phenol and phenol derivatives at the air/water interface,[14] and Eisenthal and co-workers have used second harmonic generation spectroscopy to determine the spectrum of *N*,*N*′-diethyl-*p*-nitroaniline (DEPNA) at the air/water interface[15] and at the water/1,2-dichloroethane (DCE) interface.[16]

One of the major goals of these and similar studies is to use the extensive knowledge about the relationship between solvent effects on electronic spectra and solute/solvent interactions[2,17] developed from studies in bulk liquid to gain an understanding of the nature of the microscopic environment at liquid interfaces. As has been the case in studies of bulk liquids, an important component of the study of electronic spectroscopy at interfaces is to derive simple expressions for the effect of the inhomogeneous environment on the spectra. For example, increasing the polarity of the solvent environment will lower the transition energy from the ground state to the excited state if the latter has a larger electric dipole moment. Thus, it would be useful to relate the shift in the peak spectrum at the interface relative to the spectrum in bulk liquids to the dielectric property of the liquids and the position and orientation of the solute molecule.

Besides the practical use of continuum electrostatic models of electronic spectra at interfaces, these models can help provide a simple theoretical interpretation of a large amount of experimental data. For example, recent experimental measurements of electronic spectra at several liquid/liquid interfaces suggest that the peak spectrum at the interface is very close to the average shift in the two bulk media.[16] Could this surprising result be explained using simple continuum models? Molecular dynamics simulations of electronic spectra at liquid interfaces recently reported by us[18,19] show that the spectra are quite sensitive to the location of the probe. Can this effect be understood quantitatively by continuum models?

In this paper, a continuum electrostatic model for calculating the spectral line shape at liquid interfaces and surfaces is developed. Although continuum models of liquid interfaces have been used in the past to compute ionic adsorption free energy[20] and reorganization free energy for electron transfer,[21−24] they have not been utilized to compute electronic spectral line shape. As in these models, the interface is described as a mathematically ideal plane separating two bulk dielectric media. However, unlike most applications to ET at interfaces, the model described here allows for all possible solute locations at the interface. The underlying theory and the specifics of the model are discussed in section II. The model is applied to the spectrum of DEPNA at the water liquid/vapor interface and at the water/DCE interface in sections III.A and III.B. Although the resulting model requires numerical techniques, a simple approximate analytical expression is also developed in section IIIC. Summary and conclusions are given in section IV.

II. Theory

A. Statistical Mechanical Background. The system under consideration consists of a single solute molecule (the chromophore) in a bath of solvent molecules. $V_1(\mathbf{r})$ denotes the total adiabatic potential energy of the system when the chromophore is in its ground electronic state, and $V_2(\mathbf{r})$ denotes the corresponding one for the excited state. $\mathbf{r}$ corresponds to the

10.1021/jp982058u CCC: $15.00
Published on Web 08/25/1998

positions of all solvent and solute atoms. Included in $V_1(\mathbf{r})$ and $V_2(\mathbf{r})$ is the fixed gas phase energy difference between the solute's electronic states. In the Frank−Condon approximation, the electronic absorption spectrum results from "vertical" transitions between the ground state and the excited state of the solute. Assuming that the transition dipole moment is independent of solute and solvent positions, the absorption line shape in the inhomogeneous limit (infinite excited state lifetime) is given by the ensemble average:

$$I_{1\to 2}(\omega) = \langle \delta[\omega - \Omega(\mathbf{r})] \rangle_1 = \frac{\int \delta[\omega - \Omega(\mathbf{r})] e^{-\beta V_1} \, d\mathbf{r}}{\int e^{-\beta V_1} \, d\mathbf{r}} \quad (1)$$

where $\hbar\Omega(\mathbf{r}) = V_2 - V_1$ is the energy difference between the excited and ground states at a given atomic configuration, $\beta = 1/kT$, δ is the Dirac delta function, and the energy units are such that $\hbar = 1$. Replacing the delta function by its integral representation ($\delta(x) = \int_{-\infty}^{\infty} e^{-ixt} dt$) and performing a cumulant expansion, one finds that, to second order, the line shape is given by a Gaussian,[25,26]

$$I_{1\to 2}(\omega) = \frac{1}{\sqrt{2\pi\sigma_1^2}} e^{-(\omega-\omega_1)^2/2\sigma_1^2} \quad (2)$$

where

$$\omega_1 = \langle \Omega(\mathbf{r}) \rangle_1$$

$$\sigma_1^2 = \langle [\Omega(\mathbf{r}) - \omega_1]^2 \rangle_1 \equiv \langle [\Omega(\mathbf{r})]^2 \rangle_1 - \omega_1^2 \quad (3)$$

If the transition between the two electronic states is the result of a charge transfer, one can use the formalism of electron transfer reactions to quantify the energetics involved. To this end, it is useful to define solvent free energy functions for the two electronic states.[27−29] Taking $X(\mathbf{r}) = V_2(\mathbf{r}) - V_1(\mathbf{r})$ as the "solvent coordinate", the reversible work required to produce a given solvent polarization (which corresponds to the value $X(\mathbf{r}) = x$) for the system in the ith electronic state is

$$A_i(x) = -\beta^{-1} \ln \langle \delta[X(r) - x] \rangle_i \quad (4)$$

relative to some standard state. The reorganization free energy for the state i is defined as the free energy associated with changing the solvent coordinate from $X_i = \langle X(\mathbf{r}) \rangle_i$ (which is the equilibrium value of $X(\mathbf{r})$ in the state i) to the equilibrium value of $X(\mathbf{r})$ in the second state. Thus,

$$\lambda_1 = A_1(X_2) - A_1(X_1)$$

$$\lambda_2 = A_2(X_1) - A_2(X_2) \quad (5)$$

Note that the equilibrium value X_i is simply the peak of the spectrum $\hbar\omega_i$ in the Gaussian approximation. It is important to stress that λ is a free energy difference that involves one nonequilibrium state. In contrast, the equilibrium free energy difference between the two states is given by

$$\Delta A_{1\to 2} = -\beta^{-1} \ln \frac{\int e^{-\beta V_2} \, d\mathbf{r}}{\int e^{-\beta V_1} \, d\mathbf{r}} = -\beta^{-1} \ln \langle e^{-\beta(V_2 - V_1)} \rangle_1 \quad (6)$$

After simple manipulations of the delta function in eq 4 and using eqs 5 and 6, one finds that[29]

$$X_1 = \Delta A_{1\to 2} + \lambda_2 \quad (7)$$

This simple relation, with its obvious geometric interpretation given in Figure 1, gives the peak spectrum in terms of the reorganization free energy and the reaction free energy for the corresponding ET reaction. Although the relationship given in eq 7 does not assume a Gaussian distribution of the random variable $X(\mathbf{r})$, the identification of $X_1 = \langle X(\mathbf{r}) \rangle_1$ with $\hbar\omega_i$ was based on the second-order expansion of eq 1 for the line shape. If we adopt this approximation for eq 4, we find that

$$\lambda_i = \frac{(X_2 - X_1)^2}{2\beta\sigma_i^2} \quad (8)$$

From eq 7 we find that $X_1 + X_2 = \lambda_1 + \lambda_2$, and combining this relation with eq 8 gives

$$\sigma_i = \frac{\lambda_1 + \lambda_2}{\sqrt{2\beta\lambda_i}} \quad (9)$$

which expresses the width of the absorption spectrum in terms of the reorganization free energy for the forward and backward ET reactions. Linear response theory assumes that $\lambda_1 = \lambda_2 = \lambda$, which simplifies eq 9 to give

$$\sigma_1 = \sigma_2 = \sqrt{\frac{2\lambda}{\beta}} \quad (10)$$

This equation was first derived by Marcus using a different approach.[30]

Calculating the reorganization free energy and the solvation free energy from realistic Hamiltonians is a formidable statistical mechanical task that has been attempted for bulk liquids only.[31] Thus, other than using computer simulations, the other option for computing the spectra at liquid interfaces is to use a continuum electrostatic model.

B. Continuum Electrostatic Model for $\Delta A_{1\to 2}$ and λ. Equations 7 and 10 express the peak position and width of the spectrum in terms of the reorganization free energy and the solvation free energy. These can be evaluated by the following equations using continuum electrostatics:[32]

$$\lambda = \frac{1}{8\pi} \oint [\epsilon^{o}(\mathbf{E}_2^{o} - \mathbf{E}_1^{o})^2 - \epsilon^{s}(\mathbf{E}_2^{s} - \mathbf{E}_1^{s})^2] \, d\mathbf{r} \quad (11)$$

$$\Delta A_{1\to 2} = A_2^{eq} - A_1^{eq}$$

$$A_1^{eq} = \frac{1}{8\pi} \oint [\epsilon^{s} \mathbf{E}_i^{s} \cdot \mathbf{E}_i^{s}] \, d\mathbf{r} \quad (12)$$

where ϵ^m is the dielectric constant of the medium; $m = 0$ or s, standing for the optical and static dielectric constants; and $\mathbf{E}_i^m$ is the electric field induced in this medium by the charge distribution of the ith electronic state. The calculation of the volume integrals in eqs 11 and 12 is straightforward in a homogeneous medium. For interfacial systems, one must specify a proper model for the solute and the dielectric constants. A simple and widely used choice is to model the interface as an ideal plane perpendicular to the Z-axis and located at $Z = 0$ separating two bulk homogeneous media. ϵ_{I}^m is the dielectric constant for medium I (which occupies the $Z < 0$ region), and ϵ_{II}^m is the dielectric constant for medium II. The solute is described by two nonoverlapping spherical cavities of radii a and b. The two cavities have point charges of magnitude $\pm Q_1$

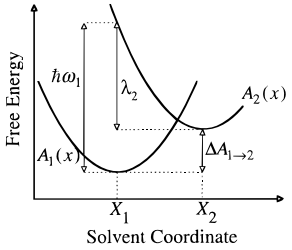

Figure 1. A schematic representation of the free energy associated with electron transfer and optical electronic transitions.

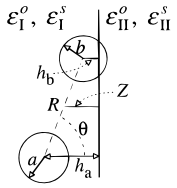

Figure 2. A schematic representation of one possible orientation of the chromophore (represented by a pair of spherical cavities with point charges) at the interface between two dielectric media.

in the ground electronic state and $\pm Q_2$ in the excited state. The two cavities may have a large number of distinct locations relative to the interface plane, depending on the location of their centers (both centers may be in one medium or each center may be in a different medium) and whether or not the interface plane goes through none, one, or both cavities. One possible location is depicted in Figure 2.

Approximate analytical expressions for the reorganization free energy and the solvation free energy for an ion pair at the liquid/liquid interface was first calculated by Kharkats[21] for the case where the centers of the two cavities are located along the line perpendicular to the interface. Marcus has extended these calculations to the three-dimensional case, [23] assuming that each cavity is wholly restricted to one medium and can't cross the interface. Thus the orientation of the vector connecting the two cavities is restricted to an angular cone whose size depends on the size of the cavities and the distance R between their centers. Benjamin and Kharkats[24] have calculated the reorganization free energy for all possible locations in 3D by numerically evaluating the integral in eq 11. These results, together with a similar approach for calculating the solvation free energy in eq 12, are used here to compute the electronic line shape.

The electric fields in eqs 11 and 12 are determined from the potential $\phi(\mathbf{r})$ generated by the charge distribution in each electronic state using $\mathbf{E} = -\nabla\phi$. The potential due to a particular charge distribution can be written as a sum of the contributions from all point charges. The potential at any point which is a distance r away from the point charge q, which is located in region I a distance h from the interface, is given by[33]

$$\phi = \begin{cases} \dfrac{q}{\epsilon_I}\left(\dfrac{1}{r} + \dfrac{1\epsilon_I - \epsilon_{II}}{r'\epsilon_I + \epsilon_{II}}\right), & \text{in region I} \\ \dfrac{q}{r\epsilon_I + \epsilon_{II}}\dfrac{2}{}, & \text{in region II} \end{cases} \tag{13}$$

where r' is the distance from the point of interest to the image point of the charge. A similar expression in which "I" and "II" are interchanged may be written if the charge is located in region II. To use the potential of the charge distribution, one may replace the volume integrals in eqs 11 and 12 by surface integrals using the identity $\int[(\nabla\phi)\cdot(\nabla\phi)]dV = \oint(\phi\nabla\phi)\cdot d\mathbf{S}$, which is correct in the region of zero charge[33] (the region outside the cavities). Specifically, consider the general volume integral $J = (1/8\pi)\oint[\epsilon\mathbf{E}\cdot\mathbf{E}]d\mathbf{r}$. Each of the integrals in eqs 11 and 12 can be written as a sum of expressions like J for each electronic state and for the optical and the static response. The equivalent surface integral can be written as a sum over the surface of all the spherical cavities. Each cavity can be either totally in medium I, or totally in medium II, or partially in both media. If S_I^j is the part of the jth spherical cavity in medium I and S_{II}^j is the part of the jth spherical cavity in medium II, then

$$J = \frac{1}{8\pi}\sum_j\left(\epsilon_I \oint_{S_I^j} \phi_I^j \nabla\phi_I^j \, d\mathbf{S} + \epsilon_{II} \oint_{S_{II}^j} \phi_{II}^j \nabla\phi_{II}^j \, d\mathbf{S}\right) \tag{14}$$

where ϕ_I^j is the electric potential on the portion of cavity j that is in region I due to all the charges in region I and their images in region II (as given by eq 13). Similarly, ϕ_{II}^j is the electric potential on the portion of cavity j that is in region II due to all the charges in region II and their images in region I.

Because of the form of the potential in eq 13, each surface integral in eq 14 can be written as a sum of terms of the form:

$$\oint_S \frac{1}{r_\alpha}\nabla\frac{1}{r_\beta} d\mathbf{S} = \int_{z_{min}}^{z_{max}} dz \int_0^{2\pi} d\varphi \frac{\sigma^2 - y_\beta\sqrt{\sigma^2 - z^2}\sin\varphi - z_\beta z}{r_\alpha r_\beta^3} \tag{15}$$

where $r_\alpha^2 = \sigma^2 + y_\alpha^2 + z_\alpha^2 - 2y_\alpha\sqrt{\sigma^2 - z^2}\sin\varphi - 2z_\alpha z$, with a similar expression for r_β^2. The surface integral is over a spherical section $\mathbf{S}$ whose radius is $\sigma = a$ or b. The limits of the integral over z, z_{min} and z_{max}, are determined by the distance h_σ of the center of the cavity from the interface. For example, if the sphere's center is in region I, the limits of the integral over the part of the sphere that is in region I are $z_{min} = -\min(h_\sigma,\sigma)$, $z_{max} = \sigma$, and the limits are $z_{min} = -\sigma$, $z_{max} = -\min(h_\sigma,\sigma)$ over the other part. The integral in eq 15 is evaluated numerically using a two-dimensional Gaussian quadrature. Examples of the explicit expressions for the integrals that contribute to the reorganization free energy and the solvation free energy for the particular configuration of Figure 2 are given in the appendix. A listing of all the cases, in the form of computer code that evaluates the electronic line shape, can be obtained from the author. web site: *http://www.chemistry.ucsc.edu/benjamin/research/codes.html.*

C. The Spectral Line Shape. As will be demonstrated below, for a chromophore model consisting of two spherical cavities, the reorganization free energy and the solvation free energy in eq 7 depend on the position Z and the orientation θ of the solute relative to the interface. Z is the distance between the center of mass and the interface, and θ is the angle between the solute dipole and the normal to the interface. Because we are interested in the electronic line shape at a given distance Z, an ensemble average over the different orientations must be performed. If

$$\Delta E_{1\to 2}(Z,\theta) = \Delta A_{1\to 2}(Z,\theta) + \lambda(Z,\theta) \tag{16}$$

is the energy difference for a given Z and θ, the linear response approximation for the line shape at this Z and θ is given by

$$I(\omega,Z,\theta) = \sqrt{\frac{\beta}{4\pi\lambda(Z,\theta)}}\exp\left\{-\frac{\beta[\omega - \Delta E(Z,\theta)]^2}{4\pi\lambda(Z,\theta)}\right\} \tag{17}$$

To obtain the orientational average line shape, we use:

$$\bar{I}(\omega,Z) = \frac{\int_0^{\pi} e^{-\beta A_1(Z,\theta)} I(\omega,Z,\theta) \sin\theta \, d\theta}{\int_0^{\pi} e^{-\beta A_1(Z,\theta)} \sin\theta \, d\theta} \qquad (18)$$

where $A_1(Z,\theta)$ is the free energy of the ground state given in eq 12. This integral can also be evaluated numerically at each value of Z.

III. Results and Discussion

A. Absorption Line Shape at the Water Liquid/Vapor Interface. A typical application of continuum electrostatics to electronic spectra in bulk liquids involves estimating the excited state dipole moment of a chromophore from a series of spectra taken in different liquids. The cavity size is regarded as a free parameter, although estimates of this quantity from molecular size have also been attempted. Here one first finds the best cavity size that reproduces the peak position of the experimental absorption line shape of DEPNA in bulk water and then uses this cavity size to study the spectrum at the interface. The values of the ground and excited state dipole moments of this chromophore are taken from a recent fit of molecular dynamics simulations to the experimental spectra in bulk water.[19]

Using this approach, the following parameters were found to give a reasonable fit of the peak position of the spectrum of DEPNA in bulk water, and they are used in the calculations reported below. The chromophore is represented by two spheres of identical radius $a = b = 2.64$ Å. The distance between the centers of these two spheres is $R = 6$ Å. The charges in the ground and excited states are $q_1 = 0.35e$ and $q_2 = 0.70e$, respectively. For the calculations at the water liquid/vapor interface, the dielectric constants of the two media used are $\epsilon^o_{liq} = 1.78$, $\epsilon^s_{liq} = 78$, $\epsilon^o_{vap} = \epsilon^s_{vap} = 1$, and the temperature is $T = 298$ K.

Figure 3 presents the results of the calculations with the above parameters. In part A, the solvent contribution to the free energy of the ground state is shown as a function of the position and orientation of the pair of charges. The angle θ is measured between the line connecting the two charges (which corresponds to distance R in Figure 2) and the normal to the interface (the chromophore is parallel to the interface when $\theta = 90$). Obviously, there is no orientation dependence when the solute center of mass is in the bulk water phase ($Z \ll 0$) or the gas phase ($Z \gg 0$), but it is interesting to note that the bulk behavior of water is already achieved at $Z = -6$ Å. In contrast, there is a strong orientation dependence near the interface. The solute prefers to be parallel to the interface when it is on the water side, and perpendicular to the interface when it is on the vapor side. The strong orientation dependency will markedly influence the weighting of the contribution of different orientations to the absorption line shape (see below). The excited state solvation free energy as a function of Z and θ will have the same exact shape as that of the ground state, but with a larger energy scale because of the larger charge. Indeed, according to eq 24 (in the appendix), for the present solute model: $A_2 = Q_2^2/Q_1^2 A_1$.

Part B gives the reorganization free energy for the "electron transfer" reaction $A^{Q_1}B^{-Q_1} \rightarrow A^{Q_2}B^{-Q_2}$. Here again there is a significant orientation dependence. When the solute is on the liquid side of the interface, the reorganization free energy of the parallel orientation is greater than that of the perpendicular orientation. The behavior is opposite when the solute is on the vapor side of the interface. Because the transition energy is $\Delta E_{1\rightarrow 2} = \Delta E_{gas} + A_2 - A_1 + \lambda$, the behavior of λ as a function of θ will make the orientation dependence of $\Delta E_{1\rightarrow 2}$ similar to, but somewhat weaker, than that of the solvation free energy.

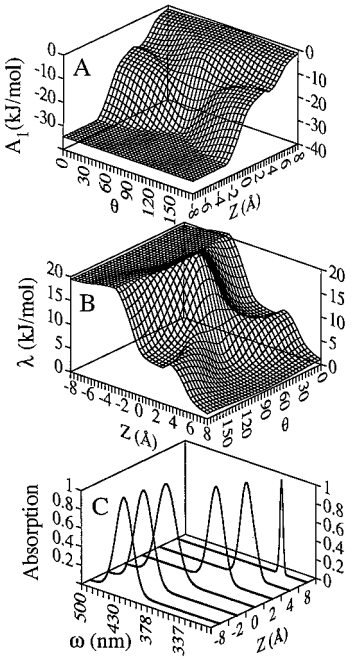

Figure 3. Calculated solvent contribution to ground state free energy (A), the reorganization free energy (B), and the orientationally averaged absorption line shape (C) for DEPNA at the water liquid/vapor interface. The line shape is normalized at each position and the frequency scale is linear in energy, not wavelength.

Given $\Delta E_{1\rightarrow 2}(Z,\theta)$, one may now calculate with the aid of eq 17 the absorption spectrum at each Z and θ and, more importantly, the orientationally weighted spectrum. This is shown in part C, where the spectral line shapes (calculated using eq 18) are given at $Z = -8$, -2, 0, 2, 4, and 8 Å. First, the spectrum in the bulk peaks at the value of $\omega_{max} = 428.4$ nm, in agreement with the experimental value of $\omega_{max} = 429$ nm. (Recall that the radius of the cavity was selected to give this value.) The width of the line shape (half-width at half-height) is $\Delta\omega = 18$ nm. The experimental value is about $\Delta\omega = 30$ nm. This discrepancy is probably due to other broadening mechanisms (vibronic, lifetime) which are missing from the current treatment, as well as to higher order corrections to the expansion in eq 1 that leads to the Gaussian expression in eq 2. The current model gives rise to a delta function lineshape in a vacuum (note the narrow lineshape at $Z = 8$ Å), and the underestimation of the width in the bulk is therefore not surprising.

As one moves from bulk water to the interface, there is a slow shift to the blue in the peak position, in agreement with experiments. Although the shift is monotonic, it significantly accelerates as the chromophore crosses the interface. This marked sensitivity to the location of the probe is a direct consequence of the discontinuous jump in the dielectric properties of the medium. Because of the rapid change in the peak position near the interface, it is somewhat difficult to compare the result with the experimental value. The experimental value[15] of $\omega_{max} = 377$ nm is reproduced if one takes the position of the chromophore to be $Z = 1.5$ Å, which is slightly into the vapor phase. Experimentally, the second harmonic signal is produced by all the molecules in the interface which are distributed according to their adsorption free energy profile. If one uses the electrostatic free energy of adsorption from the model to ascertain the average peak position, the result is near $\omega_{max} = 390$ nm. However, this neglects the hydrophobicity of

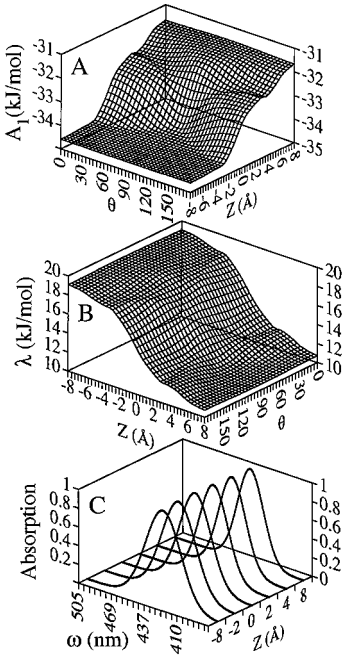

Figure 4. Same as in Figure 3 for DEPNA at the water/DCE interface.

the probe, which when properly taken into account should increase the weight of those probe locations which give rise to smaller values (blue shifted) for the peak position. Thus, one can conclude that, for this case, the continuum model gives qualitatively reasonable results for the frequency shift of the electronic absorption spectrum.

B. Absorption Line Shape at the Water/1,2-Dichloroethane Interface. The same parameters used in the previous section are used here, except that instead of water vapor the second medium is bulk DCE, for which $\epsilon^o_{DCE} = 2.5$, and $\epsilon^s_{DCE} = 10$. Note that although the static dielectric constant of the second medium (DCE) is significantly smaller than that of water, it is much larger than in the previous case. In addition, the optical dielectric constant is larger than that of water. Both of these will affect the spectrum in a significant way.

Figure 4 is analogous to Figure 3. It shows the (total) solvent contribution to the solvation free energy of the ground state (A), the reorganization free energy (B), and the electronic spectrum for the same chromophore parameters at the water/DCE interface. The solvation free energy is entirely determined by the static dielectric constants of the two liquids, and thus the general shape and the qualitative behavior are similar to the plot obtained at the water liquid/vapor interface. In particular, the orientation dependence is similar: the solute prefers the parallel orientation when it is in the high dielectric medium (H_2O) and the perpendicular orientation when it is in the lower dielectric medium (DCE). However, because the Born solvation free energy is inversely proportional to ϵ^s in the bulk medium, the energy scale in panel A of Figure 4 is much reduced compared with the one in Figure 3. The electrostatic free energy of transfer between vacuum and bulk water is -35 kJ/mol compared with -3 kJ/mol from DCE to bulk water.

The changes in the reorganization free energy as the chromophore is moved to the water/DCE interface involve a delicate balance between the changes in both the static and optical dielectric constants. The reduction in λ when the solute is transferred from bulk water to bulk DCE is qualitatively the same as in the previous system, but it is less dramatic and less orientation dependent. The combined values of $A_2 - A_1$ and λ turn out to be very insensitive to the probe location because of

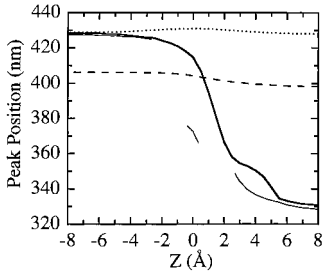

Figure 5. The peak spectrum as a function of solute position along the interface normal. Thick solid line: DEPNA at the water liquid/vapor interface. Dotted line: DEPNA at the normal water/DCE interface. Dashed line: DEPNA at the water/DCE interface in which the optical dielectric constant of both media is set to 1. Thin solid line: approximate result for DEPNA at the water liquid/vapor interface, based on an analytical expression of the energy gap.

the particular value of the solute charge. Thus, part C shows that the electronic spectrum exhibits only a very small shift (a few nm) as the probe is moved across the interface. Experimentally, the peak of the electronic absorption spectrum of DEPNA shifts from $\omega_{max} = 398$ nm in bulk DCE to $\omega_{max} = 415$ nm at the water/DCE interface to $\omega_{max} = 429$ nm in bulk water. The small interfacial effect is simply the result of the overestimation of the spectral shift in DCE. The fundamental problem is that the cavity size is selected to match the spectrum in bulk water, and the different solvation structure of DEPNA in DCE must result in a different sized cavity. Indeed, in typical applications of continuum models to the calculation of electronic spectra, the cavity size is taken to be solvent dependent. Additional support for this view comes from recent molecular dynamics calculations of the electronic spectrum of DEPNA at the water/DCE interface,[19] which are in good agreement with experiments. In this molecular model, the cavity size estimated from the radial distribution functions is indeed larger in DCE. It is of course possible to modify the continuum model to take into account the different cavity sizes in each liquid if each cavity does not cross the interface. However, as will be clear below, most of the changes in the spectrum relative to the bulk come from configurations in which at least one of the cavities is located partially in both media.

Figure 5 summarizes the main results discussed above by showing the peak position of the spectrum as a function of probe location along the interface normal. In addition to clearly summarizing the results discussed above, it also shows the data for the artificial case where both the water and DCE optical dielectric constants are taken to be 1. The result of this calculation (shown as the dashed line) clarifies the importance of the optical response of the liquids. The entire difference between this case and the normal water/DCE system is in making the reorganization free energy larger by a factor of almost two. In addition to the obvious shift to lower energies that this makes, the omission of the optical response makes the DCE phase less polar and results in a more significant variation of the transition energy and the peak position with the location of the probe.

C. An Approximate Analytical Model. A simple analytical expression for the energy gap $\Delta E_{1\rightarrow 2}$ can be derived if one assumes that no cavity can be located partially in one medium. As a result, for the case of a dumbbell solute (AB) with cavities of sizes a and b which are separated by a distance R, there is a restriction put on the allowed values of the distance Z between the center of the AB bond and the interface. Three cases can be identified: (i) $Z < -\min(a,b)$; both cavities are in medium I. All the values of the angle θ between the interface normal

and the solute bond are allowed if $Z < -\max(a,b)$. (ii) $|Z| < R/2 - \max(a,b)$; one cavity is in medium A and the other in medium B. In this case the values of the angle θ are restricted for each Z. (iii) $Z > \min(a,b)$; both cavities are in medium II.

Marcus[23] derived a simple analytical expression for A_1, A_2, and λ for the second case. Using the same approach, the expressions for A_1, A_2, and λ in the other two cases, (i) and (iii), can be easily determined. The complete result for the energy gap for all cases is

$$\Delta E_{1\rightarrow 2} = (q_2 - q_1)^2(I_o - I_s) + (q_2^2 - q_1^2)(I_s - 1/2a - 1/2b) \tag{19}$$

where

$$I_m = \frac{1}{2\epsilon_{\mathrm{I}}^m a} + \frac{1}{2\epsilon_{\mathrm{II}}^m b} + \frac{\eta_m}{4\epsilon_{\mathrm{I}}^m h_a} - \frac{\eta_m}{4\epsilon_{\mathrm{II}}^m h_b} - \frac{2}{R(\epsilon_{\mathrm{I}}^m + \epsilon_{\mathrm{II}}^m)},$$

(A in I and B in II)

$$= \frac{1}{2\epsilon_{\mathrm{I}}^m}\left[\frac{1}{a} + \frac{1}{b} + \frac{\eta_m}{2h_a} + \frac{\eta_m}{2h_b} - \frac{1}{R} - \frac{\eta_m}{\sqrt{R^2/4 + h_a h_b}}\right],$$

(A and B in I) (20)

and $\eta_m = (\epsilon_{\mathrm{I}}^m - \epsilon_{\mathrm{II}}^m)/(\epsilon_{\mathrm{I}}^m + \epsilon_{\mathrm{II}}^m)$ with obvious permutations of "I" and "II" for the other two possibilities (A in "II" and B in "I" or A and B in "II"). Because the derivation of eq 19 neglects certain finite-sized effects, there is a small difference between this expression and the numerical results obtained earlier in the region where eq 19 applies, but the difference is quite small (less than 1% for the water/DCE system). However, because of the strong angular dependence near the interface, the spectral line shape calculated using eqs 17−20 will differ from the numerical one for solutes located very near the interface, especially for a system where the dielectric constant of the two media is very different. This is shown in Figure 5 for the water liquid/vapor interface. The thin solid line is the peak spectrum calculated from the analytical expression (compared with the thick solid line determined numerically). The thin line is discontinuous because for $R/2 < |Z| < a$ one or both cavities crosses the interface and the approximate solution is not valid. The numerical and analytical results agree well for locations far from the interface, but there is significant deviation as one approaches the interface, especially in case ii. Interestingly, and fortuitously, the approximate analytical result for this case agrees far better with the experimental value ($\omega_{\max} = 377$ nm) than does the exact numerical value.

IV. Conclusions

The continuum electrostatic model for calculating the electronic absorption line shape at liquid interfaces discussed in this paper provides a convenient route for estimating interfacial effects on spectral features. It is in reasonable agreement with experimental data and molecular dynamics simulations, although it also highlights the problems inherent in continuum models of the interface.

The model takes into account the finite size of the solute cavity and all its possible locations relative to the interface, treating it as a fixed parameter. The model could be improved in several ways, including by using different sized cavities for the solute in different media and by introducing surface roughness and more complicated cavity shapes. Although it is expected that all of these will improve the comparison with experimental results (especially using variable size cavity), these additions also involve using a larger number of parameters and therefore represent a substantial increase in the complexity of the model.

Acknowledgment. This work has been supported by a grant from the National Science Foundation. (CHE-9628072)

Appendix

Given here are the formulas for the integrals that appear in the expression of the solvation free energy and the reorganization free energy for the system depicted in Figure 2. The electrostatic potential at any field point in regions I and II is

$$\phi_{\mathrm{I}}^m = \frac{q}{\epsilon_{\mathrm{I}}^m}\left(\frac{1}{r_a} + \frac{\eta_m}{r_a'} - \frac{1}{r_b} - \frac{\eta_m}{r_b'}\right) \equiv q\zeta_{\mathrm{I}}^m$$

$$\phi_{\mathrm{II}}^m = \frac{2q}{\epsilon_{\mathrm{I}}^m + \epsilon_{\mathrm{II}}^m}\left(\frac{1}{r_a} - \frac{1}{r_b}\right) \equiv q\zeta_{\mathrm{II}}^m \tag{21}$$

where $m = o$, s and $\eta_m = (\epsilon_{\mathrm{I}}^m - \epsilon_{\mathrm{II}}^m)/(\epsilon_{\mathrm{I}}^m + \epsilon_{\mathrm{II}}^m)$. The distances r_a and r_a' are between any field point and the center of sphere A and its image, respectively, and similarly for sphere B (see Figure 2). Next one defines

$$\psi_A^m = \oint_A \zeta_{\mathrm{I}}^m \nabla\zeta_{\mathrm{I}}^m \cdot \mathrm{d}\mathbf{S}_A$$

$$\psi_{B_{\mathrm{I}}}^m = \oint_{B_{\mathrm{I}}} \zeta_{\mathrm{I}}^m \nabla\zeta_{\mathrm{I}}^m \cdot \mathrm{d}\mathbf{S}_B \tag{22}$$

$$\psi_{B_{\mathrm{II}}}^m = \oint_{B_{\mathrm{II}}} \zeta_{\mathrm{II}}^m \nabla\zeta_{\mathrm{II}}^m \cdot \mathrm{d}\mathbf{S}_B$$

where $d\mathbf{S}_A = 2\pi\mathbf{r}_a dz$, $d\mathbf{S}_B = 2\pi\mathbf{r}_b dz$, with $\mathbf{r}_a$ and $\mathbf{r}_b$ being vectors from the center of each sphere to a point on the surface of that sphere. Each one of the integrals in eq 22 can be written as a sum of the expressions given in eq 15 and thus reduced to a quadrature. Using $q = Q_1$ and $q = Q_2$ for the ground and excited states of the solute, respectively, one finally obtains

$$\lambda = \frac{(Q_2 - Q_1)^2}{8\pi}[\epsilon_{\mathrm{I}}^o \psi_A^o + \epsilon_{\mathrm{I}}^o \psi_{B_{\mathrm{I}}}^o + \epsilon_{\mathrm{II}}^o \psi_{B_{\mathrm{II}}}^o - \epsilon_{\mathrm{I}}^s \psi_A^s - \epsilon_{\mathrm{I}}^s \psi_{B_{\mathrm{I}}}^s - \epsilon_{\mathrm{II}}^s \psi_{B_{\mathrm{II}}}^s] \tag{23}$$

$$A_i^{\mathrm{eq}} = \frac{Q_i^2}{8\pi}[\epsilon_{\mathrm{I}}^s \psi_A^s + \epsilon_{\mathrm{I}}^s \psi_{B_{\mathrm{I}}}^s + \epsilon_{\mathrm{II}}^s \psi_{B_{\mathrm{II}}}^s] \quad i = 1, \text{or } 2 \tag{24}$$

References and Notes

(1) Suppan, P.; Ghoneim, N. *Solvatochromism*; The Royal Society of Chemistry: Cambridge, 1997.
(2) Reichardt, C. *Solvents and Solvent Effects in Organic Chemistry*, 2nd ed.; VCH: Weinheim, 1988.
(3) Ågren, H.; Mikkelsen, K. V. *J. Mol. Struct. (THEOCHEM)* **1991**, *234*, 425.
(4) Shemetulskis, N. E.; Loring, R. F. *J. Chem. Phys.* **1991**, *95*, 4756.
(5) Bader, J. S.; Berne, B. J. *J. Chem. Phys.* **1996**, *104*, 1293.
(6) Stephens, M. D.; Saven, J. G.; Skinner, J. L. *J. Chem. Phys.* **1997**, *106*, 2129.
(7) Matyushov, D. V.; Schmid, R.; Ladanyi, B. M. *J. Phys. Chem. B* **1997**, *101*, 1035.
(8) McRae, E. G. *J. Phys. Chem.* **1957**, *61*, 562.
(9) Bakhshiev, N. G. *Opt. Spektrosk.* **1964**, *16*, 821.
(10) Mirashi, L. S. P.; Kunte, S. S. *Spectrochimica Acta* **1989**, *45A*, 1147.
(11) Dey, J.; Dogra, S. K. *J. Phys. Chem.* **1994**, *98*, 3638.
(12) Karpovich, D. S.; Blanchard, G. J. *J. Phys. Chem.* **1995**, *99*, 3951.
(13) Saroja, G.; Samanta, A. *Chem. Phys. Lett.* **1995**, *246*, 506.

(14) Tamburello-Luca, A. A.; Hébert, P.; Brevet, P. F.; Girault, H. H. *J. Chem. Soc., Faraday Trans.* **1996**, *92*, 3079.
(15) Wang, H.; Borguet, E.; Eisenthal, K. B. *J. Phys. Chem.* **1997**, *101*, 713.
(16) Wang, H.; Eisenthal, K. B. *Abstracts of Papers*, 214th National Meeting of the American Chemical Society, Las Vegas, NV, Fall 1997; American Chemical Society: Washington, DC, 1997.
(17) Reichardt, C. *Chem. Rev.* **1994**, *94*, 2319.
(18) Michael, D.; Benjamin, I. *J. Chem. Phys.* **1997**, *107*, 5684.
(19) Michael, D.; Benjamin, I. *J. Phys. Chem.* **1998**, in press.
(20) Benjamin, I. *Annu. Rev. Phys. Chem.* **1997**, *48*, 401.
(21) Kharkats, Y. I. *Elektrokhimiya* **1976**, *12*, 1370.
(22) Kharkats, Y. I.; Volkov, A. G. *J. Electroanal. Chem.* **1985**, *184*, 435.
(23) Marcus, R. A. *J. Phys. Chem.* **1990**, *94*, 1050, 4152.
(24) Benjamin, I.; Kharkats, Y. I. *Electrochimica Acta* **1998**, in press.
(25) Kubo, R. *J. Phys. Soc. Jpn.* **1962**, *17*, 1100.
(26) Mukamel, S. *Principles of Nonlinear Optical Spectrocopy*; Oxford: New York, 1995.
(27) Warshel, A. *J. Phys. Chem.* **1982**, *86*, 2218.
(28) Carter, E. A.; Hynes, J. T. *J. Phys. Chem.* **1989**, *93*, 2184.
(29) King, G.; Warshel, A. *J. Chem. Phys.* **1990**, *93*, 8682.
(30) Marcus, R. A. *J. Chem. Phys.* **1965**, *43*, 1261.
(31) Zhou, Y.; Friedman, H. L.; Stell, G. *Chem. Phys.* **1991**, *152*, 185.
(32) Marcus, R. A. *J. Chem. Phys.* **1963**, *38*, 1858.
(33) Jackson, J. D. *Classical Electrodynamics*; Wiley: New York, 1963.